

# ALMA Resolves the Stellar Birth Explosions in Distant Radio-Loud Quasars

Peter Barthel<sup>1</sup>  
José Versteeg<sup>1,2</sup>

<sup>1</sup> Kapteyn Astronomical Institute,  
University of Groningen,  
the Netherlands

<sup>2</sup> Department of Astrophysics/IMAPP,  
Radboud University, Nijmegen,  
the Netherlands

Far-infrared photometry with the Herschel Space Observatory has found many examples of ultra-luminous dust emission at around 40 K in the host galaxies of high-redshift, radio-loud 3C Active Galactic Nuclei (AGN). The dust heating could have its origin in the central black hole activity or extreme circumnuclear starbursts, or both. We have used the Atacama Large Millimeter/submillimeter Array (ALMA) in Cycle 3 to study the dust morphology on the kiloparsec scale in a sample of these AGN, and present the results for three well-known distant quasars: 3C298, 3C318, and 3C454. After correction for the non-thermal radiation at 1 mm, the observations imply a starburst origin for the cool thermal dust emission, and a symbiotic physical relationship with the AGN-driven radio source.

## The starburst-AGN symbiosis in distant 3C radio source hosts

Given the well-known scaling relations between galaxies and their central black holes, galaxies are believed to experience star formation, i.e., converting gas into stars, and central black hole growth, specifically AGN phenomena, symbiotically. This symbiosis is indeed seen in observations; nearby quasi-stellar objects (QSOs), for instance, prefer blue host galaxies (Trump et al., 2013). The symbiosis of black hole and global galaxy growth is even more intriguing because of the possible feedback effects: positive (AGN-induced star formation), and/or negative (AGN quenching of star formation). Concerning these feedback effects, the class of radio-loud AGN is particularly interesting since these objects — radio galaxies and radio-loud quasars — have radio jets which are known to interact with the host galaxy interstellar medium (ISM). The

physical AGN–star formation interplay is an issue of great interest: where, when and how does it occur? To answer these questions, it is necessary to zoom in on the star formation processes in the host galaxies of radio-loud AGN and to conduct a spatial and/or kinematic study of the astrophysical interconnections.

During the past decade our team has used Spitzer, Chandra, and Herschel to investigate partly obscured AGN and star formation in the ultra-massive hosts of  $z > 1$  3C radio galaxies and quasars (for example, Barthel et al., 2012; Podigachoski et al., 2015, 2016a). These objects have been and will continue to be landmarks in the study of active galaxies through cosmic time. Herschel photometry has shown that about a third of these powerful 3C AGN are in fact radio-loud Ultra Luminous InfraRed Galaxies (ULIRGs) as inferred from their large cool dust masses, suggesting star formation rates (SFRs) of hundreds to over a thousand  $M_{\odot} \text{ year}^{-1}$ . Key questions focus on the nature of this cool dust and its location; is it widespread in the AGN host galaxy and indeed related to massive starbursts, or is it localised and maybe somehow connected to the active nucleus?

Our Herschel studies have also established the interesting trend that the cool dust luminosity is a function of the AGN age (Podigachoski et al., 2015), in the sense that old AGN — large double-lobed radio sources — are characterised by less dust emission than young ones with compact, sub-galactic-sized radio sources. Within the starburst scenario, this would indicate positive feedback during the young AGN phase and negative feedback during its adult phase, or simply fading of the galaxy growth over time. A similar trend was recently reported for high-redshift radio galaxies (Falkendal et al., 2019).

## Zooming in using ALMA 1-millimetre observations

In 2016 ALMA was capable of 0.15-arcsecond resolution imaging at a wavelength of 1 mm, and hence permitted a spatial study of star formation related to cool dust on kiloparsec scales. This high resolution also permits optimal subtraction

of the co-spatial non-thermal (synchrotron) 1-millimetre emission, using scaled high-resolution centimetre radio images; this is essential to isolate the thermal emission and address its nature.

ALMA Band 7 (1-millimetre) observations of five, far-infrared (FIR) luminous,  $z > 1$  3C objects — three quasars and two radio galaxies — took place during the summer of 2016, with baselines of up to 1.6 km, and a typical on-source integration time of 15 minutes. Standard CASA pipeline calibration was employed at the European ALMA Regional Centre Node in Leiden, the Netherlands. The resulting beam sizes are typically 0.18 arcseconds, and the final 1-millimetre images reach  $1\sigma$  noise levels of a few tens of  $\mu\text{Jy beam}^{-1}$ .

As millimetre radiation from the nucleus of a radio-loud object consists of two parts: the thermal Rayleigh-Jeans tail of the cool (30–40 K) host galaxy dust component, and the synchrotron component of its radio source — the strength of which can be extrapolated from the shape of its centimetre radio spectrum. There is also a third component in the form of free-free radiation, but its magnitude is not significant at the rest-frame wavelength of 0.4 mm (Condon, 1992).

To establish the strength and morphology of the cool dust thermal emission in the quasar hosts, that is its Rayleigh-Jeans tail at 1 mm, we combined our ALMA images with the Karl G. Jansky Very Large Array (VLA) *U*-band (2 cm, 15 GHz) images at matched angular resolution ( $\sim 0.18$  arcseconds), subtracting a scaled, aligned version of the latter from the former. Gaia positions of the optical QSOs permitted high-precision astrometric alignment of the images, to within one 0.025-arcsecond pixel. We will describe the analysis of these quasars below; the full sample including the radio galaxies will be discussed in a forthcoming article (and quasar 3C298 was already discussed in Barthel et al., 2018).

## Three well-known 3C quasars and their central dust structures

Within our Cycle-3 ALMA project (ADS/JAO.ALMA#2015.1.00754.S), three 3C quasars were observed: 3C298

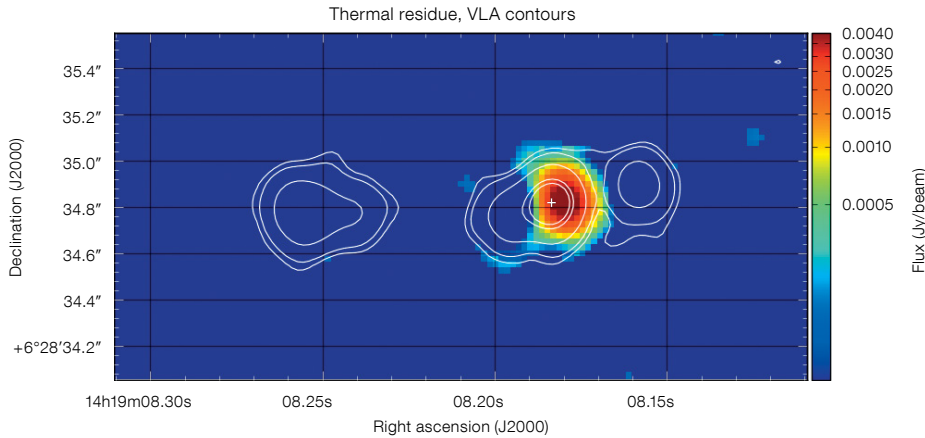


Figure 1. Thermal dust emission at 1 mm in the host galaxy of 3C298, with 2-centimetre radio contours overlaid; the + sign marks the location of the optical QSO.

at  $z = 1.439$ , 3C318 at  $z = 1.574$ , and 3C454.0 at  $z = 1.757$ . Their (projected) radio sizes are, respectively, 14, 10 and 10 kpc, hence they are of sub-galactic dimensions and most likely young. Their model-dependent (see Podigachoski et al., 2015) star formation rates (SFRs), as inferred from their spectral energy distributions (SEDs), are 940, 580 and 620  $M_{\odot} \text{ year}^{-1}$ , respectively. Our SED greybody fits to the long-wavelength FIR data predicted thermal 1-millimetre flux densities of 3, 1.5, and 1.5 mJy, for 3C298, 3C318 and 3C454.0, respectively. The ALMA observations were designed to test the SED modelling, specifically to identify or rule out the presence of these massive starbursts, to determine their strength, and to study any astrophysical interconnection with the AGN. The results of this study are discussed separately for each quasar.

3C298 is a compact triple radio source, consisting of a radio core coinciding with the AGN, a western radio lobe 0.4 arcseconds away, and an eastern lobe 1 arcsecond away. The optical QSO is slightly reddened and it displays strong associated CIV absorption from outflowing winds (Anderson et al., 1987). 3C298 is one of the strongest FIR emitters in the 3C catalogue. Its 1-millimetre ALMA image has the triple structure, but the central emission shows evidence of an extended underlying 1-millimetre plateau.

We used an accurately aligned, archival VLA 2-centimetre image at comparable resolution to subtract the non-thermal 1-millimetre emission. Since the non-thermal 2-centimetre to 1-millimetre spectral indices for the various source components are unknown *a priori* we used a range of indices (scaling factors) in the subtraction process. Over-subtracting non-thermal centrally peaked emission creates a hole in the central 1-millimetre structure; we conclude that adopting a synchrotron spectral index value of  $-1$  yields the best “organic” thermal 1-millimetre morphology, shown in Figure 1 with the 2-centimetre radio contours overlaid. That structure, having a 1-millimetre flux density of around 3 mJy, represents roughly 16% of the core emission in 3C298 and thereby provides an excellent fit to the 38 K grey-body fit of Podigachoski et al. (2015). We observe strong dust emission towards the nearby western radio lobe, as well as a clump of faint dust emission at the location of the jet deflection, south-east of the core/AGN. The dust is likely linked to the optical disturbance in the 3C298 host galaxy observed by the HST (Hilbert et al., 2016) and to the CO disc reported by Vayner et al. (2017).

The compact (1.2-arcsecond double) radio source 3C318 was originally thought to be an extremely bright FIR source, but the Herschel imaging of Podigachoski et al. (2016b) showed that a substantial fraction of the FIR flux originates from a foreground pair of interacting galaxies. Nevertheless, the updated FIR data still suggest a SFR of 580  $M_{\odot} \text{ year}^{-1}$ , from model-dependent SED fitting. At 0.18-arcsecond resolution,

our ALMA 1-millimetre image shows a somewhat resolved core structure of 2.2 mJy integrated strength. As seen from 0.03-arcsecond resolution MERLIN+EVN radio imaging (Spencer et al., 1991), the compact radio double breaks up into a multi-component structure at a position angle of 45 degrees.

We obtained VLA Director’s Discretionary Time (DDT) observations in 2018 to image 3C318 at 2 cm, permitting us to subtract the non-thermal emission from the 1-millimetre image, at the ALMA resolution, after careful alignment of the images. The resulting thermal residue, with radio contours overlaid, is shown in Figure 2; residual thermal emission is seen immediately north-east and south-west of the AGN core, with a total 1-millimetre flux density of 0.23 mJy, which is 11% of the total 1-millimetre flux density. These dust features are perfectly aligned with the elongated, multicomponent, cm-wavelength radio emission, hence their morphology and strength provide strong support for the circumnuclear starburst picture.

Quasar 3C454.0 displays a bent, sub-arcsecond-sized radio source. We obtained archival VLA 2-centimetre data, yielding an image at a resolution comparable to our ALMA 1-millimetre image, which we subtracted from the latter, after accurate alignment and flux density scaling. The resulting residual thermal 1-millimetre emission, overlaid with the VLA 2-centimetre radio contours, is shown in Figure 3; it is concentrated just east of the optical AGN, elongated roughly north-south, and peaking at the location of the bend in the radio structure. Its integrated strength is 1.9 mJy, which is 18% of the total 1-millimetre flux density. These values do not change the SED-inferred SFR (Podigachoski et al., 2015); they in fact support the circumnuclear starburst picture.

### Radio-loud ULIRGs, their ISM, and feedback mechanisms

In summary, all three sample quasars — having compact, subgalactic-sized radio morphologies and strongly suspected to have high SFRs — were found to possess circumnuclear dust structures on

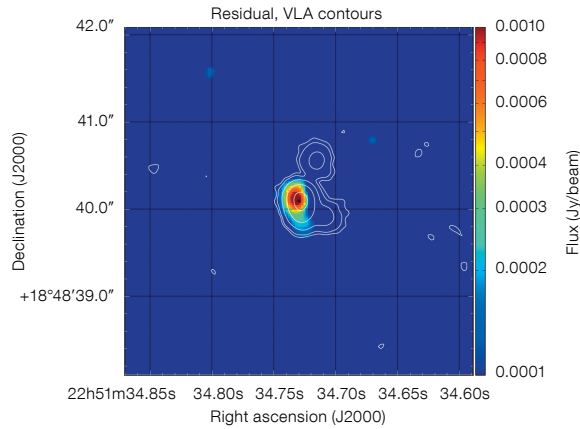
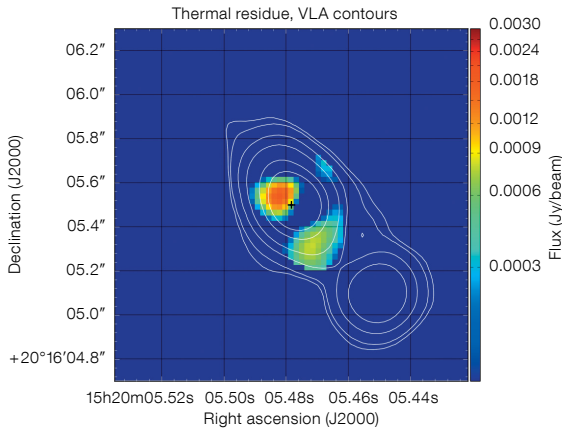


**Figure 2. (far left)** Thermal dust emission at 1 mm in the host of 3C318, with 2-centimetre radio contours overlaid; the + sign marks the location of the optical QSO.

**Figure 3. (left)** Thermal dust emission at 1 mm in the host of 3C454.0, with 2-centimetre radio contours overlaid; the + sign marks the location of the optical QSO.

the subarcsecond (kpc) scale. The ALMA resolution of roughly 0.18 arcseconds seems to be crucial to isolating these structures in the 1-millimetre images, which are otherwise dominated by nuclear synchrotron (non-thermal) radiation. The dust morphologies are indicative of radio jet–ISM interaction, and their ULIRG-strength FIR luminosities find a natural explanation in positive AGN feedback, i.e., extra-strength star-formation, driven by the advancing radio jets in the dense central parts of the AGN hosts. In other words, these AGN – which are most likely young – present evidence for positive rather than negative feedback.

What about negative feedback – does the present study shed light on that mechanism? We believe it does, but the negative feedback appears to be starburst- rather than AGN-driven. One of the sample quasars, 3C298, displays outflowing gas winds, seen as so-called associated CIV absorption in the optical QSO spectrum, but also from other ions and molecules, as observed with integral field spectroscopy by Vayner et al. (2017). As we have argued elsewhere (Barthel et al., 2017), there is evidence that such quasar winds have their origin in massive ongoing host starbursts, such as observed locally in Messier 82; 3C298 would be a prime example of such starburst-driven negative feedback. On the other hand, we cannot rule out AGN quenching in more mature and old radio sources (see, for example, Falkendal et al., 2019).

Confirming the intermediate-resolution study of extreme-redshift QSOs by Wang et al. (2013), we find from our high resolu-

tion imaging that the symbiotic dusty starbursts are very compact circumnuclear structures, extending a few kiloparsecs from the AGN at most. This is in agreement with the lower-resolution Atacama Compact Array study of FIR-bright SDSS QSOs (Hatziminaoglou et al., 2018). Such compact starbursts have also been observed in luminous submillimetre galaxies (for example, Tacconi et al., 2006; Hodge et al., 2016; Calistro-Rivera & Hodge, 2018), so they may be one and the same phenomenon building up massive galaxies, regardless of whether there is active massive black hole (MBH) accretion or not.

Finally, our identification of the cool dust emission as originating from a starburst gives confidence that the mechanism is the hitherto tacitly assumed source of the long-wavelength far-infrared emission (that is to say in the SED modelling – for example, Barthel et al., 2012; Leipski et al., 2014; Ma & Yan, 2015; Podigachoski et al., 2015; Pitchford et al., 2016; Westhues et al., 2016). Given the frequent incidence of ultraluminous  $\sim 40$ -K dust emission in high-redshift AGN, the symbiotic occurrence of starbursts and black hole buildup must be widespread.

### To be continued

These intriguing observations call for several follow-up studies. Firstly, higher-resolution ALMA 1-mm imaging is now possible, permitting the examination of the morphological details of the jet-star formation interaction. Secondly, ALMA spectroscopy can determine the kinemat-

ics of the gas involved in the feedback mechanism, including the postulated starburst-driven superwinds. Thirdly, control samples of low-SFR 3C AGN, in compact, young as well as large, mature radio sources, must be studied with ALMA and compared with the high-SFR objects. Concerning the more distant future, JWST imaging may reveal the newly formed circumnuclear star clusters.

### Acknowledgements

We acknowledge our long-time collaborators Pece Podigachoski, Martin Haas and Belinda Wilkes for exciting years of study of an exciting AGN sample. Thanks are also due to our ALMA project co-I's Carlos De Breuck and George Djorgovski, to the VLA Director for granting us DDT time in 2018, and to Jack Radcliffe for data processing advice. Finally, the assistance of the Netherlands ALMA Regional Center is gratefully acknowledged.

### References

- Anderson, S. F. et al. 1987, *AJ*, 94, 278
- Barthel, P. D. et al. 2012, *ApJ*, 757, L26
- Barthel, P. D. et al. 2017, *ApJ*, 843, L16
- Barthel, P. D. et al. 2018, *ApJ*, 866, L3
- Calistro-Rivera, G. & Hodge, J. 2018, *The Messenger*, 173, 33
- Condon, J. J. 1992, *ARA&A*, 30, 575
- Falkendal, T. et al. 2019, *A&A*, 621, A27
- Hatziminaoglou, E. et al. 2018, *MNRAS*, 480, 4974
- Hilbert, B. et al. 2016, *ApJS*, 225, 12
- Hodge, J. A. et al. 2016, *ApJ*, 833, 103
- Leipski, C. et al. 2014, *ApJ*, 785, 154
- Ma, Z. & Yan, H. 2015, *ApJ*, 811, 58
- Pitchford, L. K. et al. 2016, *MNRAS*, 462, 4067
- Podigachoski, P. et al. 2015, *A&A*, 575, A80
- Podigachoski, P. et al. 2016a, *MNRAS*, 462, 4183
- Podigachoski, P. et al. 2016b, *A&A*, 585, A142
- Spencer, R. E. et al. 1991, *MNRAS*, 250, 225
- Tacconi, L. et al. 2006, *ApJ*, 640, 228
- Trump, J. R. et al. 2013, *ApJ*, 763, 133
- Vayner, A. et al. 2017, *ApJ*, 851, 126
- Wang, R. et al. 2013, *ApJ*, 773, 44
- Westhues, C. et al. 2016, *AJ*, 151, 120